UPPSALA UNIVERSITET

INVIVE-Approx

Simulating the human respiratory system from an approximation perspective

Elisabeth Larsson, Scientific Computing, Uppsala University, Sweden

Credit goes to the INVIVE team

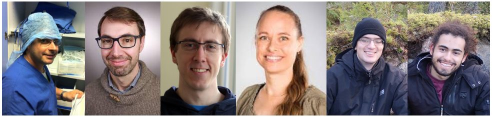

Nicola Cacciani | Pierre Villard | Igor Tominec | Ulrika Sundin | Boštjan Mavrič | Andreas Michael

Workshop on Multivariate Approximation and Geometric Modelling, Moscow, Nov 30, 2021

Ventilator induced diaphragmatic dysfunction

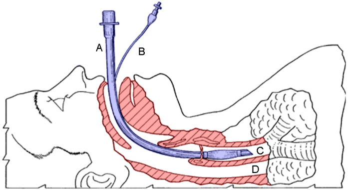

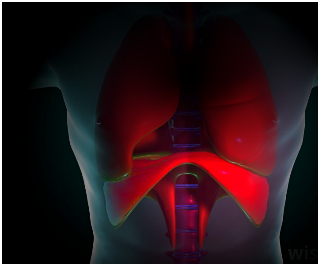

- Mechanical ventilation of intensive care patients leads to *Ventilator induced diaphragmatic dysfunction* (VIDD).
- In normal breathing the diaphragm contracts, but ventilation stretches the muscle.
- Significant loss off function in short time, $\mathcal{O}(24h)$.
- Goal: Understand effect, reduce effect, plan rehabilitation.

The INVIVE project

Application: Biomechanical modeling of the respiratory system to evaluate and improve mechanical ventilation.

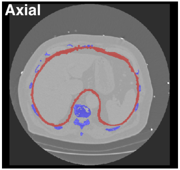

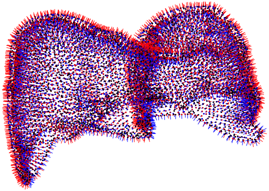

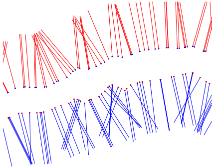

- Raw geometry data—3D medical images.
- Segmented data—Noisy and locally biased.
- Pressure, volume and geometry time series data.

Desired outcomes:

- Smooth geometry reconstruction.
- Simulation of muscle tissue during ventilation.

UPPSALA UNIVERSITET

INVIVE-Approx

Radial basis function (RBF) approximation

Scaled translates $\varphi(\varepsilon\|\underline{x}-\underline{x}_j\|)$ of positive definite function $\varphi(r)$ such as the Gaussian.

Approximations

$$\tilde{u}(\underline{x}) = \sum_{j=1}^{N} \lambda_j \phi(\varepsilon\|\underline{x}-\underline{x}_j\|)$$

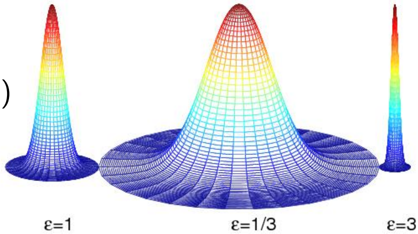

Differentiation

$$\mathcal{L}\tilde{u}(\underline{y}) = \sum_{j=1}^{N} \lambda_j \mathcal{L}\phi(\varepsilon\|\underline{y}-\underline{x}_j\|)$$

Advantages

- Meshfree - flexible with respect to geometry.
- Spectrally accurate approximations.
- Ease of implementation.

Geometry design objectives and approach

UPPSALA
UNIVERSITET

INVIVE-Approx

The surface representation

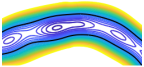

- Implicit surface given by zero level set.
- Localized approximations to keep cost low.
- Infinitely smooth representation (globally).
- No spurious zero level sets.

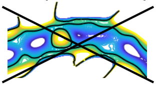

Approach to reach target

- Decouple basis location from data.
- Anisotropic local approximations.
- Extra stabilizing conditions.

UPPSALA
UNIVERSITET

INVIVE-Approx

Partition of unity method for thin structures

- Global approximation $\tilde{u}(\underline{x}) = \sum_{j=1}^{P} w_j(\underline{x})\tilde{u}_j(\underline{x})$
  P – the number of patches
  w_j – partition of unity weight function
  $\tilde{u}_j$ – patch local radial basis function approximation
- One layer of cylindrical patches.
- The patches are adapted to the geometry.

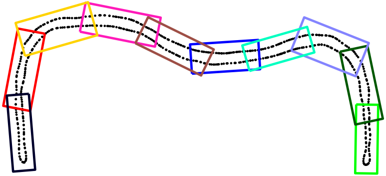

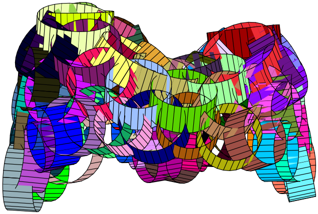

UPPSALA UNIVERSITET

INVIVE-Approx

The adaptive cover generation

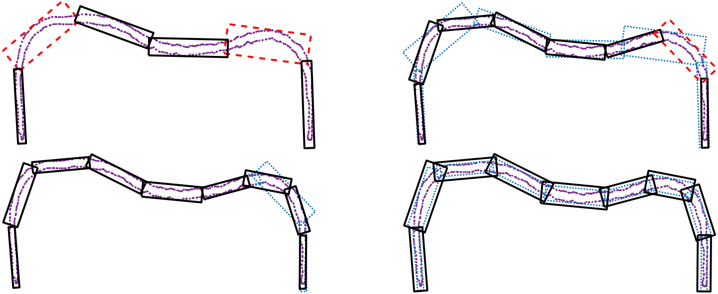

- Initial clustering of points using `kmeans`.
- Cylindrical patches are fitted to the data using PCA.
- Thick patches (large curvature) are subdivided.
- Finally an overlap δ is enforced between patches.

Partition of unity weight functions

Cylindrical reference patch with radius R and height H.

Choose a basic function $\begin{cases} \psi_0(r) >, 0 & 0 \leq r < 1, \\ \psi_0(r) = 0, & r \geq 1. \end{cases}$

Local generating function $\psi(\underline{x}') = \psi_0\left(\frac{r'}{R}\right)\psi_0\left(\frac{x'_d}{H/2}\right)$ positive on the patch and zero on the patch boundary.

Normalize with Shepard's method $w_j(\underline{x}) = \frac{\psi_j(\underline{x})}{\sum_{k=1}^{P}\psi_k(\underline{x})}$.

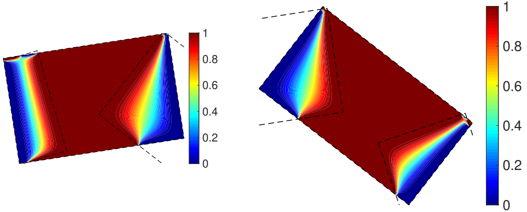

Overlap determines gradients. Non-smooth at outer boundary intersections.

UPPSALA UNIVERSITET

INVIVE-Approx

The local geometry approximations

RBF approximation of local level set function

$$s(\underline{x}') = \sum_{j=1}^{n_c} \mu_j \phi(\|\underline{x}' - \underline{x}_j'\|).$$

Multiquadric RBFs
$\phi(r) = \sqrt{1 + r^2}$.

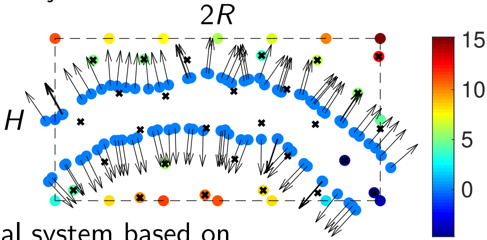

Overdetermined local system based on

- Zero value at data points.

  (Some points outside are included.)

- Unit component in normal direction.
- Additional distance values.

Effects of method parameters

Parameters: The number of RBFs n_c, ref patch H, R.

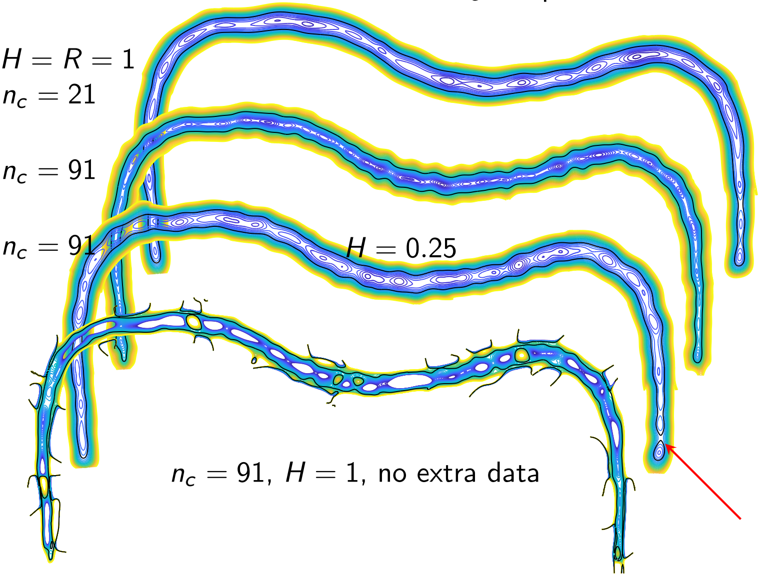

Smooth geometry reconstruction

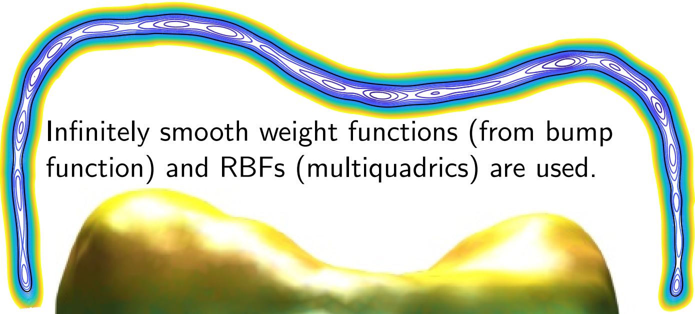

Infinitely smooth weight functions (from bump function) and RBFs (multiquadrics) are used.

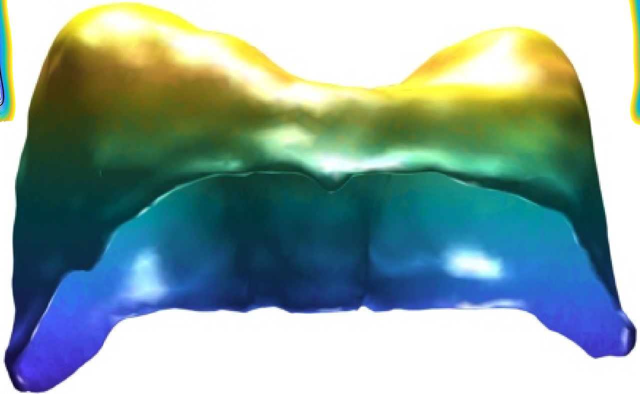

UPPSALA UNIVERSITET

INVIVE-Approx

Solving a PDE in the diaphragm geometry

Challenges

- Complex, thin, non-parametric geometry.
  Representation, resolution, node generation.
- Pressure conditions on large parts of the boundary.
  Conditioning/sensitivity to node layout.

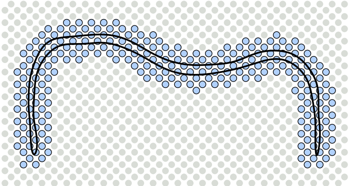

Solution approaches

- Oversampled RBF methods for stability.
  RBF-PUM: Larsson, Shcherbakov Heryudono 2017.
  RBF-FD: Tominec, Larsson, Heryudono 2021.
- Unfitted RBF methods for nodes and resolution.
  Tominec, Breznik 2021.

Oversampled RBF-FD

For a point $\underline{x}_c$ pick $n \ll N$ neighbours $\underline{x}_j$, $j = 1, \ldots, n$
We interpolate $u(\underline{x}_j)$ using $\phi(r) = r^3$ and monomials p_j

$$\tilde{u}(\underline{x}) = \sum_{j=1}^{n} \lambda_j \phi(\|\underline{x} - \underline{x}_j\|_2) + \sum_{j=1}^{m} \mu_j p_j(\underline{x})$$

under the constraint $\sum_{j=1}^{n} \lambda_j p_k(\underline{x}_j) = 0$, $k = 1, \ldots, m$.

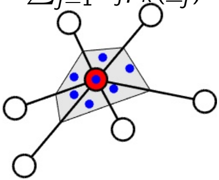

We enforce the PDE and boundary conditions at points $\underline{y}$ in the Voronoi region around $\underline{x}_c$

$$\mathcal{L}\tilde{u}(\underline{y}) = \sum_{j=1}^{n} \lambda_j \mathcal{L}\phi(\|\underline{y} - \underline{x}_j\|_2) + \sum_{j=1}^{m} \mu_j \mathcal{L} p_j(\underline{y}).$$

Continuous least-squares approximation for Poisson with mixed boundary conditions

Continuous norm and homogeneous space

L_2-norm $\|u\|_\Omega^2 = (u,u)_{L_2(\Omega)} = \int_\Omega |u(y)|^2\,dy$.

$V^0 = \{v \in W_2^2(\Omega) \,:\, v|_{\partial\Omega_D} = 0\}$.

Least-squares for the PDE problem

Minimize $\|\Delta u - f\|_\Omega^2 + \|\frac{\partial u}{\partial n} - g\|_{\partial\Omega_N}^2 + \|u - h\|_{\partial\Omega_D}^2$.

Write as: $u \in V$ such that $a(u,v) = \ell(f,v)$, $\forall v \in V$,

where $a(u,v) = (\Delta u, \Delta v)_\Omega + (\frac{\partial u}{\partial n}, \frac{\partial v}{\partial n})_{\partial\Omega_N} + (u,v)_{\partial\Omega_D}$.

Coercivity of the bilinear form

$$C^2 a(v,v) \geq \|v\|_\Omega^2, \quad v \in V^0.$$

UPPSALA UNIVERSITET

INVIVE-Approx

Discrete $\leftrightarrow$ semi-discrete

Let v_h be the discontinuous RBF-FD-LS approximation and define a fully discrete norm from

$$(f,g)_{\ell_2(\Omega)} = \frac{|\Omega|}{M}\sum_{i=1}^{M} f(y_i)g(y_i).$$

This is a discretization of the semi-discrete inner product

$$(f,g)_{L_2^*(\Omega)} = \sum_{k=1}^{N}(f,g)_{L_2(\mathcal{V}_k)} \quad (\mathcal{V}_k \text{ Voronoi regions}),$$

$$\|v_h(Y)\|_{\ell_2(\Omega)} \leq (1+\tau)\|v_h\|_{L_2^*(\Omega)},$$

$$a^*(v_h,v_h) \leq \frac{1}{(1-\tau)} a_h(v_h,v_h).$$

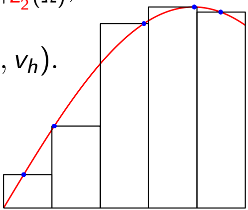

τ is small when M is large enough.

Semi-discrete $\leftrightarrow$ continuous

Let $v = S(v_h) \in W_2^2(\Omega)$ be the smoothed counterpart of v_h
We can show that

$$\|v_h\|^2_{L_2^*(\Omega)} \leq (1+\eta_0)\|v\|^2_{L_2(\Omega)},$$

$$a(v,v) \leq (1+\eta_a)a^*(v_h,v_h).$$

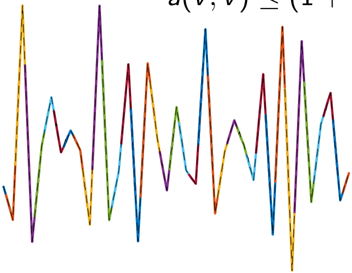

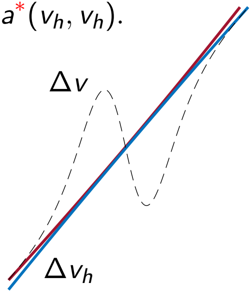

η_0 and η_a in practice become smaller with smoother data, but do not depend on the oversampling M.

UPPSALA UNIVERSITET

INVIVE-Approx

Stability estimate: Coercivity

$$
\begin{aligned}
\|v_h\|^2_{\ell_2(\Omega)} &\le (1+\tau)\|v_h\|^2_{L_2^*(\Omega)} \\
&\le (1+\tau)(1+\eta_0)\|v\|^2_{L_2(\Omega)} \\
&\le (1+\tau)(1+\eta_0)C^2 a(v,v) \\
&\le (1+\tau)(1+\eta_0)C^2(1+\eta_a)a^*(v_h,v_h) \\
&\le \frac{(1+\tau)(1+\eta_0)C^2(1+\eta_a)}{1-\tau} a_h(v_h,v_h).
\end{aligned}
$$

τ—quadrature error, decreases with # equations M.

η_0, η_a—smoothing errors, decrease with smoothness.

C—coercivity bound for functions in $W_2^2(\Omega)$, fixed.

Convergence: Consistency

- Polynomial basis of degree K, $m = \frac{(K+1)\cdots(K+d)}{d!}$.
- Stencil size $n \geq 2m$, larger if skewed.
- Well-distributed, but preferably not Cartesian nodes.

Theorem Bayona 2019

Then $|\mathcal{L}u(\underline{x}) - \sum_{j=1}^{n} \mathcal{L}\psi_j(\underline{x})| = \mathcal{O}(h^{K+1-\alpha})$, where α is the order of the operator $\mathcal{L}$, and h measures node distance.

The final convergence estimate

For a Poisson problem with Dirichlet and Neumann boundary conditions, and polynomials of degree K

$$\|e\|_{\ell_2(\Omega)} \leq \sqrt{2}C\left(\frac{(1+\tau)(1+\eta_0)(1+\eta_a)}{1-\tau}\right)^{\frac{1}{2}} (c_1h^{K+1}+c_2h^K+c_2h^{K-1})|u|_{W_\infty^{K+1}(\Omega)}.$$

- Convergence rate determined by the degree K.
- Optimal convergence requires sufficient smoothness.
- Error decreases mainly with h, but also with M^{-1}.

UPPSALA UNIVERSITET

INVIVE-Approx

Run-time comparison

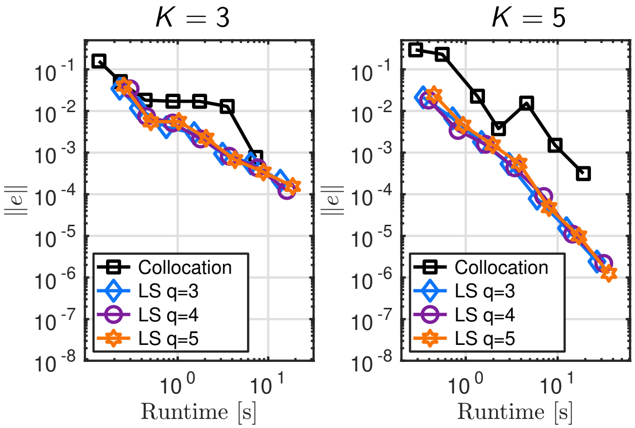

- Least-squares RBF-FD is more efficient.
- Efficiency almost independent of $M = qN$.
- High accuracy, more benefit from large K.

Linear elasticity in cross section

- Model problem: Linear elasticity with manufactured Dirichlet and traction conditions.
- Method: Oversampled RBF-FD

  Tominec, Larsson, Heryudono 2021
- Smoothed boundary conditions

  arXiv preprint: Tominec, Villard, Larsson, Bayona, Cacciani 2021

Unfitted RBF-FD on the whole diaphragm

A Poisson problem with mixed boundary conditions is solved in the diaphragm geometry.

Unfitted nodes

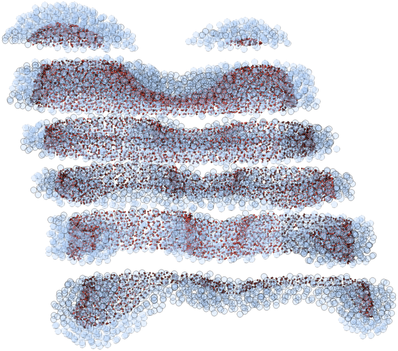

Error distribution

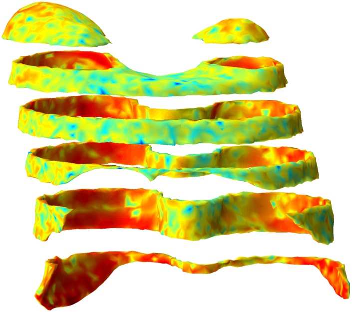

Largest error here $\approx 5 \cdot 10^{-3}$

Summary

Using localized oversampled RBF methods, we can

- reconstruct non-trivial smooth geometries in a controlled way, and
- solve PDE model problems in these geometries at a reasonable cost.

To model a real diaphragm, we further need

- a proper tissue model, including active muscle contraction, and
- real boundary conditions given by the abdominal pressure, the thoracic pressure, and the attachment to the ribs and spine.